A Monte-Carlo study for the critical exponents of the three-dimensional $O(6)$ model

D. Loison

Institut für Theoretische Physik, Freie Universität Berlin, Arnimallee 14, 14195 Berlin, Germany

Damien.Loison@physik.fu-berlin.de

and

Laboratoire de Physique Théorique et Modélisation, Université de Cergy-Pontoise, 2, Avenue Adolphe Chauvin, 95302 Cergy-Pontoise Cedex, France

dami@u-cergy.fr

Abstract

Using Wolff's single-cluster Monte-Carlo update algorithm, the three-dimensional $O(6)$-Heisenberg model on a simple cubic lattice is simulated. With the help of finite size scaling we compute the critical exponents ν, β, γ and η. Our results agree with the field-theory predictions but not so well with the prediction of the series expansions.

P.A.C.S. numbers:05.70.Fh, 64.60.Cn, 75.10.-b

I. INTRODUCTION

The static properties of the three-dimensional classical $O(N)$ ferromagnet have been studied by high-temperature series expansion techniques [1,2] and by the field-theoretical formulation of the renormalization group [3]. For $O(6)$ these results disagree with each other (see table I). We try to resolve this discrepancy by Monte-Carlo (MC) simulations which are free of systematic errors contrary to high-temperature series and field-theory where resummation techniques are used.

The main interests of studying the critical behavior of the $O(6)$ model are, first to compare the results of Monte-Carlo and the high temperature expansions and in particular to see if the corrections used in this last method, which gives correct results for low N, are reliable for higher N; second because in frustrated spin systems the cases $O(2)$ or XY-spins and $O(3)$ or Heisenberg spins are expected to be quite different from the O(6) case [4]. Before comparing the results of field theory with numerical simulations for the frustrated case [5] we want to judge the degree of confidence obtainable by both methods in studying the less controversial ferromagnetic case.

To obtain precise critical exponents we use Wolff's algorithm [6,7] which is very effective in reducing critical slowing down. This method allows us to cover the whole region in the spin space which is much more important in the $O(6)$ case than in the $O(2)$ or $O(3)$ cases. This is the first use of this algorithm for high N.

In section II we present the model and details of the simulation. The thermodynamic quantities, their finite size scaling behavior and the methods to calculate the critical exponents are exposed in section III. The results are shown and discussed in section IV and the section V is devoted to the conclusion.

II. MODEL AND SIMULATION

We choose for the classical $O(6)$ model an isotropic ferromagnet on a three-dimensional simple cubic lattice. The Hamiltonian for such spin system is given by:

$$H = J \sum_{(ij)} \mathbf{S}_i . \mathbf{S}_j \tag{1}$$

where $\mathbf{S}_i$ is a six components classical vector of length unit and J is the ferromagnetic coupling constant ($J < 0$). We consider $L * L * L$ (L from 8 to 36) systems with nearest-neighbor interactions and periodic boundary conditions.

We use Wolff's single-cluster algorithm [6,7]. It has been demonstrated that this method is very effective in reducing critical slowing down for the $O(N)$ ferromagnetic spin model [9–11].

All simulations are carried out at temperatures where the finite size effects [16] are important: $0.67 < T < 0.77$ (For example with size L=10, 14 simulations at different temperatures have been done). In each simulation, at least 6 millions measurements were made after enough single cluster updating (1 million) were carried out for equilibration. For the simulations at T_c 20 millions measurements were made.

We use in this work the histogram MC technique developed by Ferrenberg and Swendsen [12,13]. From a simulation done at T_0, this technique allows to obtain thermodynamic quantities at T close to T_0. Since the energy spectrum of a Heisenberg spin system is continuous, the data list obtained from a simulation is basically a histogram with one entry per energy value. In order to use the histogram method efficiently, we divided the energy range E between -3 and 0 into 100 000 bins.

Our errors are calculated with the help of the Jackknife procedure [14].

III. FINITE-SIZE SCALING (FSS)

To begin with, we have to define the quantities we need for our analysis in the FSS region. For each temperature we calculate the following quantities

$$C = \frac{< E^2 > - < E >^2}{N k_B T^2} \tag{2}$$

$$\chi = \frac{N(< M^2 > - < M >^2)}{k_B T} \tag{3}$$

$$\chi_2 = \frac{N < M^2 >}{k_B T} \tag{4}$$

$$V_1 = \frac{< ME >}{< M >} - < E > \tag{5}$$

$$U = 1 - \frac{< M^4 >}{3 < M^2 >^2} \tag{6}$$

where T is the temperature, M the order parameter, C the specific heat per site, χ the magnetic susceptibility per site, χ_2 the magnetic susceptibility per site in the high temperature region where the order parameter is zero, V_1 is a cumulant which we use to obtain the critical exponent ν, U the fourth order cumulant, $< ... >$ means the thermal average.
Note that the order parameter M is defined in this work as

$$M = \frac{(\sum_j (\sum_i S_i^j)^2)^{1/2}}{N} \tag{7}$$

where $j = 1, ...6$ and $\sum_i$ is the sum on all sites (N).

According to the FSS theory [16,17], for a sufficiently large system at a temperature T close enough to the infinite-lattice critical point T_c one has

$$C = c_\infty(t) + L^{\alpha/\nu} \; f_C(x) \tag{8}$$

$$\chi = L^{\gamma/\nu} \; f_\chi(x) \tag{9}$$

$$\chi_2 = L^{\gamma/\nu} \; f_{\chi_2}(x) \tag{10}$$

$$V_1 = L^{1/\nu} \; f_{V_1}(x) \tag{11}$$

$$< M > \; = L^{-\beta/\nu} \; f_M(x) \tag{12}$$

where

$$x = tL^{1/\nu} = (T - Tc)L^{1/\nu} \tag{13}$$

is the temperature scaling variable. Since we will be interested only in zero-field properties, x is the only relevant thermodynamic variable. f_i are some unknown functions.

From these equations we can prove that the location of the extrema of C, χ, and V_1 vary asymptotically as

$$T_{max}(L) = T_c + aL^{-1/\nu}. \tag{14}$$

Because each thermodynamic function has its own scaling function, a depends, in magnitude and sign, on the particular function measured.

In addition, if x is constant, i.e. if $T = T_c$ $(x = 0)$ or $T = T_c + aL^{-1/\nu}$ $(x = a)$ we have

$$C = c_\infty(t) + L^{\alpha/\nu}\ g_C \tag{15}$$

$$\chi = L^{\gamma/\nu}\ g_\chi \tag{16}$$

$$\chi_2 = L^{\gamma/\nu}\ g_{\chi_2} \tag{17}$$

$$V_1 = L^{1/\nu}\ g_{V_1} \tag{18}$$

$$< M > \ = L^{-\beta/\nu}\ g_M \tag{19}$$

where the g are constants independent of temperature and size L. So we have several possibilities to calculate T_c and the critical exponents:

1. We can look at the extrema of C, χ (Fig. 7) and V_1 and get the values of $T_{max}(L)$ and of the maximum for each quantity. We can fit this last quantities with (15-19) and find the critical exponents α/ν, γ/ν, $1/\nu$ (Fig. 1-3). Usually the result for α/ν is not very accurate because of the presence of $c_\infty(t)$. With the values of ν and $T_{max}(L)$ we can find T_c using (14) (see Fig. 4).

Now we will introduce another method to find the critical exponents, in particular to find β. It is not necessary to be at the maximum of the quantity in order to obtain the behavior (15-19) which is very useful in the case of the magnetization $< M >$ and χ_2 as they do not have a maximum. To obtain the behavior (15-19) we must have the temperature T as (14). For this we have two solutions:

a. $T = T_{max}$ of one quantity and at this temperature all the other quantities have the behavior (15-19) ,

b. T is like U=constant, indeed

$$U = f_U(x) + \text{corrections} \tag{20}$$

and if we do not include the corrections, x must be constant i.e. all the quantities have the behavior (15-19).

The errors in these two cases will be greater than if we are at the maximum of the quantity we want to fit with (15-19). Indeed we do not include the corrections and we have an uncertainty about the temperature then an error in the value of the quantity at this temperature. In the case where we are at the maximum this is not so important due to the function is flat close to it. An example of this can be found in the results (22-24) and we can compare the errors between (22) and (23) where one is the result of χ at his maximum (22) and one is the result of χ_2 at the same temperature (23). We can see that the error in the last case is more important than in the first. Nevertheless this is the best way to obtain β/ν if we use only the first method. The second method we develop hereafter include the corrections.

2. Another possibility to find T_c is to use the FSS of U. We can record the variation of U with T for various system sizes and then locate the intersection of these curves. We compare the value of U for two different lattice sizes L and $L' = bL$, making use of the condition [15]

$$\left.\frac{U_{bL}}{U_L}\right|_{T=T_c} = 1. \tag{21}$$

Because of the presence of residual corrections to finite size scaling, one actually needs to extrapolate the results of this method for $(\ln b)^{-1} \to 0$ (Fig. 5-6). With the value of T_c we can find the critical exponents with (15-19).

3. A third way to find the critical exponents and T_c together is to try to collapse for each quantity the curves of all the sizes using (8-12): We have, for example, $\chi = L^{\gamma/\nu}\ f_\chi(x)$ with $x = tL^{1/\nu} = (T - Tc)L^{1/\nu}$ and if we draw $\chi L^{-\gamma/\nu}$ as function of x with the good value for T_c, $1/\nu$ and γ/ν, all the curves should collapse (Fig. 8). Unfortunately this method does not give very accurate results because we have too many parameters to fit (3, i.e T_c, γ/ν and $1/\nu$).

We will introduce now a better way to find the critical exponents. We can draw the quantities $< M > L^{\beta/\nu}, \chi L^{-\gamma/\nu} \ldots$ not as function of x but as function of U. Indeed U varies as (20)

and all the curves for different sizes L must collapse (Fig. 9). This way we have only one unknown parameter β/ν for M, γ/ν for χ and χ_2, $1/\nu$ for V_1, and the results will be much more accurate. The errors are larger than those of the method 2 because we do not include the corrections. To find T_c now, we use the value of ν found and we plot U in function of x: T_c is the only unknown parameter.

IV. RESULTS

First we estimated the critical exponents with method 1 described in the previous section. We measured the value of the maximum of χ and V_1 and plotted in Fig. 1 and 3, in a log-log scale these values as function of the size L. We obtain γ/ν and $1/\nu$ from the slope of a straight line fit. Curve 3 in the Fig. 1 gives

$$\frac{\gamma}{\nu} = 1.970(6) \ . \tag{22}$$

We can have another estimate of γ/ν if we plot χ_2 at the estimated temperature (T^{χ}_{max}) where χ is maximum. This is shown by curve 2 in the same figure. The slope of the linear fit is

$$\frac{\gamma}{\nu} = 1.963(12) \ . \tag{23}$$

The value of the error is greater than for χ because the uncertainty about T^{χ}_{max}. The value of β/ν can be determined in the same way in plotting the logarithm of the magnetization obtained at T_{max} as function of the $\ln(L)$. The value of the slope gives (bottom curve of Fig. 2)

$$\frac{\beta}{\nu} = 0.524(7) \ . \tag{24}$$

The value of ν is obtained through the same method. For V_1 we can take the value at T^{χ}_{max} or at $T^{V_1}_{max}$. In the Fig. 3 where we have plotted $\ln(V_1)$ as function of $\ln(L)$ the two values are nearly identical because T^{χ}_{max} is close to $T^{V_1}_{ext}$ and V_1 is flat between the two temperatures. From the value at T^{χ}_{max} we obtain (curve 2 in Fig. 3)

$$\nu = 0.784(9) \tag{25}$$

and with the value V_1^{max} (i.e. at $T_{max}^{V_1}$) (curve 1 in Fig. 3)

$$\nu = 0.785(7). \tag{26}$$

We can now find the critical temperature with the value of ν just calculated. We know that the maximum of the thermodynamic quantities varies as eq. (14). In plotting for each quantities T_{max} as function of $L^{-1/\nu}$ with ν =0.785 we will obtain an estimate of the T_c. This is done in Fig. 4. We notice that the T_{max}^{χ} have the smallest error bars whereas the T_{max}^{C} are not precise. If we fit the three curves, combining the results, the estimate of T_c is

$$T_c = 0.7000(2). \tag{27}$$

Another way to find T_c is to follow method 2 of the previous section. In Fig. 5 U is plotted as function of the temperature for different sizes from $L = 10$ to $L = 36$. From this data we extrapolate the value of T_c in Fig. 6 and obtain for T_c

$$T_c = 0.7001(1) \tag{28}$$

which agrees with the value estimated before. We can estimate U at T_c (U^*)

$$U^* = 0.6477(4). \tag{29}$$

With the value of T_c (28) we do some log-log fit to find the critical exponents. It should be noticed that this value of T_c takes care of corrections which have not been included before in the values of $T_{max}(L)$. We obtain from V_1 (Fig. 3 bottom curve), from χ (Fig. 1 bottom curve), from χ_2 (Fig. 1, curve 1), and from $< M >$ (Fig. 2, curve 1)

$$\nu = 0.786(5) \tag{30}$$

$$\frac{\gamma}{\nu} = 1.969(6) \tag{31}$$

$$\frac{\gamma}{\nu} = 1.965(7) \tag{32}$$

$$\frac{\beta}{\nu} = 0.520(4). \tag{33}$$

All our errors include the influence of the uncertainty in our estimate for T_c.

Now we use the method 3. In the Fig. 7 the susceptibility χ is shown with different sizes as function of the temperature. In the Fig. 8 we have plotted the quantity $\chi L^{-\gamma/\nu}$ as function of $(T - T_c)L^{1/\nu}$ for the values of the exponents and T_c found before. We can see that all curves for different sizes collapse in one curve. Meanwhile it is better to plot these curves as function of U. Fig. 9 shows $\chi L^{-\gamma/\nu}$ for $\gamma/\nu = 1.969$. We can see that the curves collapse in one curve. With this method we obtain

$$\frac{\gamma}{\nu} = 1.970(15). \tag{34}$$

This value is similar to those found before with a greater error bar. A similar method can be employed for $< M >$, χ, χ_2 ... and we recognize the same exponents as before with greater error bars.

V. CONCLUSION

Our results are given in table I. The values of α and η are derived from the scaling relations

$$d\nu = 2 - \alpha \tag{35}$$

$$\frac{\gamma}{\nu} = 2 - \eta. \tag{36}$$

In order to check the hyperscaling relation (35) we take the relation $2\beta/\nu + \gamma/\nu = d$ which is derived from (35) and $\alpha + 2\beta + \gamma = 2$. We obtain with our Monte Carlo results

$$2\frac{\beta}{\nu} + \frac{\gamma}{\nu} = 3.009(13) \tag{37}$$

which is indeed not far from $d = 3$. Also listed in the table are the results of series expansions [1,2] and field theory [3].

Our results agree very well with the field theoretical ones. The agreement is not so good with the results of the high–temperature expansions (HT). Our value of the critical

temperature T_c agrees with the HT unbiased value but not with the of θ-biased. It is to be noted that in the unbiased case the exponents are closer to ours than for the θ-biased case where sub-leading scaling corrections have been included. We believe that the results of the field theory are more accurate than those of the high temperature expansions which give systematically larger exponents for ν and γ.

VI. ACKNOWLEDGMENTS

This work was supported by the Alexander von Humboldt Foundation. I am grateful to Professor K. D. Schotte for his support, discussions and for critically reading the manuscript. I thank A. Sokolov, P. Butera and M. Comi for correspondence.

TABLES

	ν	γ	η	β	α	T_c
this work	0.786(5)	1.548(14)	0.031(5)	0.409(6)	-0.358(15)	0.7001(1)
Field theory (6-loops) [3]	0.790	1.556	0.031	0.407	-0.370	
HT sc unbiased [1,2]	0.804(3)	1.582(5)				0.69999(3)
HT sc θ-biased [1,2]	0.821(3)	1.614(5)				0.69981(3)
HT bcc unbiased [1,2]	0.796(3)	1.566(4)				
HT bcc θ-biased [1,2]	0.819(3)	1.608(4)				

TABLE I. Values of the critical exponents and the critical temperature for $O(6)$ ferromagnetic spins on cubic lattices obtained by various methods

REFERENCES

[1] P. Butera and M. Comi, Phys. Rev. B **52**, 6185 (1995)

[2] P. Butera and M. Comi, Phys. Rev. B **56**, 8212 (1997)

[3] S.A. Antonenko and A.I. Sokolov, Phys. Rev. E **51** 1894(1995)

[4] S.A. Antonenko and A.I. Sokolov, Phys. Rev. B **49** 15901(1994)

[5] D. Loison in preparation

[6] U. Wolff, Phys. Rev. Lett. **62**, 361 (1989)

[7] U. Wolff, Nucl. Phys. B **322**, 759 (1989)

[8] U. Wolff, Phys. Lett. B **222**, 473 (1989)

[9] U. Wolff, Phys. Lett. B **228**, 379 (1989)

[10] W. Janke, Phys. Lett. A **148**, 306 (1990)

[11] J.S. Wang, Physica A **164**, 240 (1990)

[12] A. M. Ferrenberg and R. H. Swendsen, Phys. Rev. Let. **61**, 2635 (1988)

[13] A. M. Ferrenberg and R. H. Swendsen, Phys. Rev. Let. **63**, 1195 (1989)

[14] B. Efron, *The Jackknife, The Bootstrap and other Resampling Plans* (SIAM, Philadelphia, PA, 1982)

[15] K. Binder, Z. Phys. B **43**, 119 (1981)

[16] Barber, *in Phase Transition and Critical Phenomena*, edited by C. Domb and J.L. Lebowitz (Academic, New York, 1983), Vol. 8

[17] A. M. Ferrenberg and D. P. Landau, Phys. Rev. B **44**, 5081 (1991)

FIGURE CAPTIONS

Fig. 1: Values of the susceptibilities χ and χ_2 as a function of L in a ln-ln scale. Curves 1 and 2 are for χ_2 at T_c and T^{χ}_{max} respectively and curves 3 and 4 for χ at T^{χ}_{max} and T_c. The slopes of curves 1, 2, 3, 4, give γ/ν= 1.965(7), 1.963(12), 1.970(6), 1.969(6). Size L=8 is not included in the fit. The estimated error bars are smaller than the symbols.

Fig. 2: Value of $< M >$ as a function of L in a ln-ln scale at T^{χ}_{max} (curve 1) and T_c (curve 2). The value of the slopes gives β/ν. We obtain 0.520(4), 0.524(7) respectively. Size L=8 is not included in the fit. The estimated error bars are smaller than the symbols.

Fig. 3: Value of V_1 as a function of L in a ln-ln scale at $T^{V_1}_{max}$ (curve 1), T^{χ}_{max} (curve 2) and T_c (curve 3). The two first curves are quasi equal (see text). The value of the slopes gives $1/\nu$ and we obtain ν= 0.785(7), 0.784(9), 0.786(5) (up to down). Size L=8 is not included in the fit. When not shown, the estimated error bars are smaller than the symbols.

Fig. 4: Size dependence of the finite-lattice effective critical temperatures estimated from V_1, χ and C for L=8, 10, 12, 14, 16, 18, 20, 30. The lines are fit to Eq. (14) with ν=0.785. The value of T_c found is 0.7000(2). The size L=8 is not included in the fit. When not shown, the estimated error bars are smaller than the symbols.

Fig. 5: Binder's parameter U as function of the temperature for different sizes L (in the left part of the figure, from L=8 - down- to L=36 - up). The arrow shows the estimated critical temperature T_c.

Fig. 6: Estimated T_c plotted vs inverse logarithm of the scale factor $b = L'/L$. For clarity, only the results for L=12,14,16 are shown. The estimated temperature is T_c=0.7001(1).

Fig. 7: χ as function of the temperature for different sizes (from up to down L= 36, 30, 24, 20, 18, 16, 14, 12, 10).

Fig. 8: $\chi L^{-\gamma/\nu}$ as function of $(T - T_c)L^{1/\nu}$ with γ/ν=1.969, T_c=0.7001 and $1/\nu$=0.786 for different sizes L. All the curves collapse to one.

Fig. 9: $\chi L^{-\gamma/\nu}$ as function of U with γ/ν=1.969, for different sizes L. All the curves collapse to one. There is now only one unknown parameter (γ/ν).

FIGURES

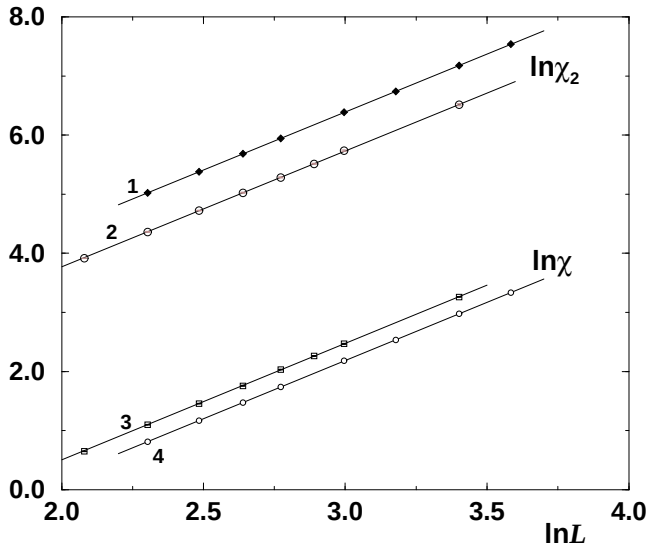

FIG. 1.

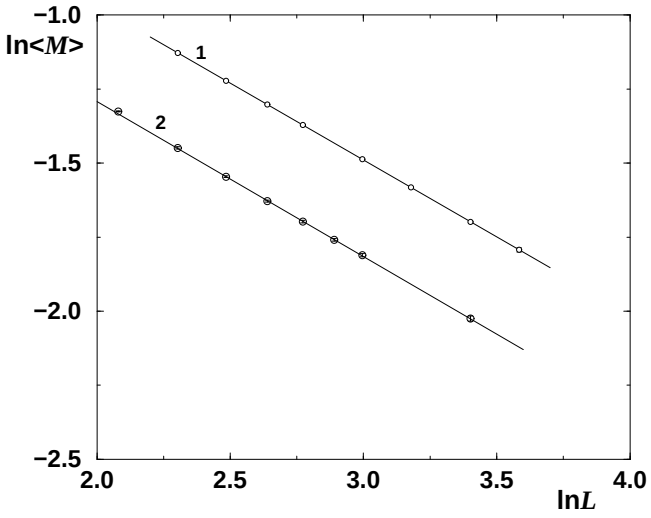

FIG. 2.

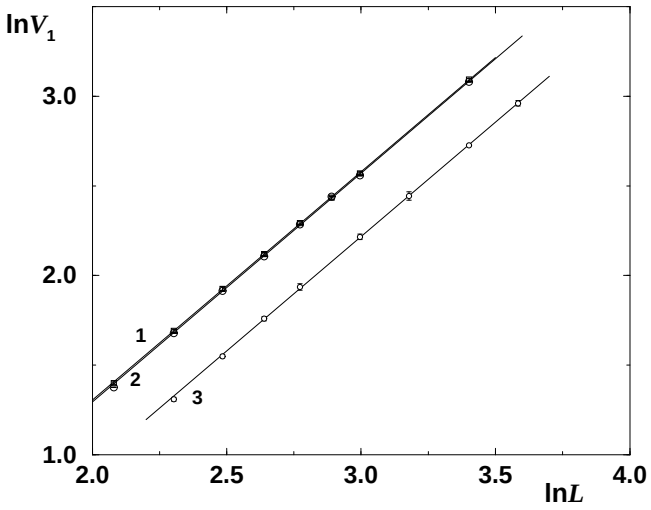
lnV_1
3.0
2.0
1.0
1
2
3
2.0
2.5
3.0
3.5
4.0
ln$L$

FIG. 3.

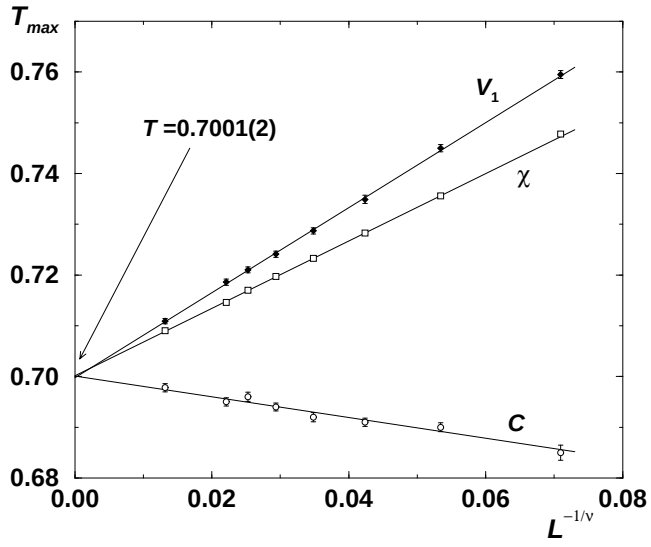
T_{max}
0.76
0.74
0.72
0.70
0.68
T =0.7001(2)
V_1
χ
C
0.00
0.02
0.04
0.06
0.08
$L^{-1/\nu}$

FIG. 4.

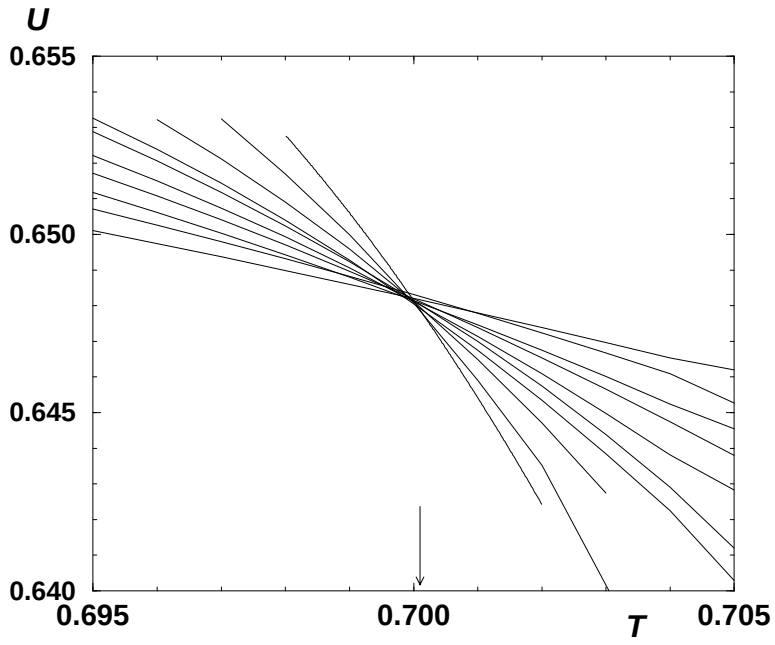
U
0.655
0.650
0.645
0.640
0.695
0.700
0.705
T

FIG. 5.

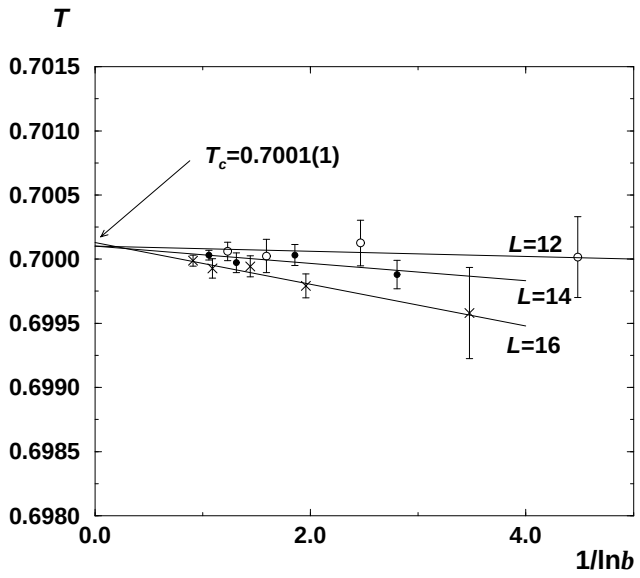
T
0.7015
0.7010
0.7005
0.7000
0.6995
0.6990
0.6985
0.6980
T_c=0.7001(1)
L=12
L=14
L=16
0.0
2.0
4.0
1/lnb

FIG. 6.

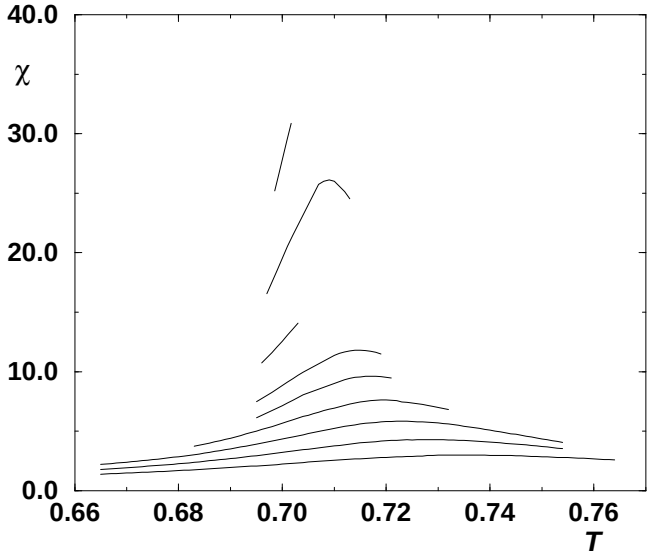
40.0
χ
30.0
20.0
10.0
0.0
0.66
0.68
0.70
0.72
0.74
0.76
T

FIG. 7.

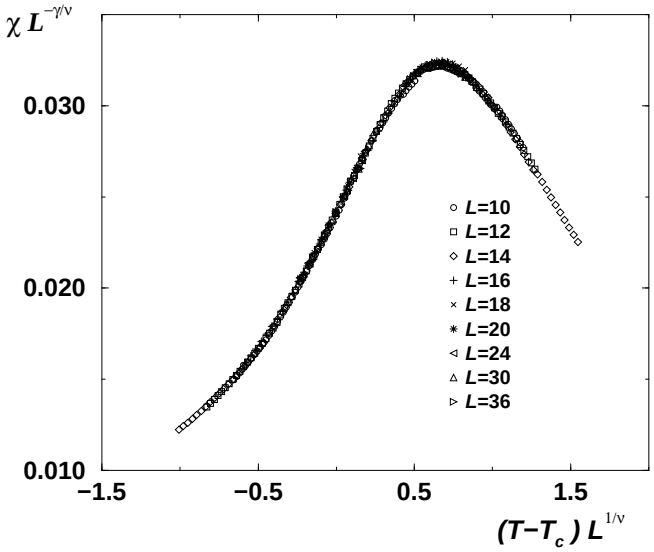
χ L^{−γ/ν}
0.030
0.020
0.010
−1.5
−0.5
0.5
1.5
(T−T_c) L^{1/ν}
L=10
L=12
L=14
L=16
L=18
L=20
L=24
L=30
L=36

FIG. 8.

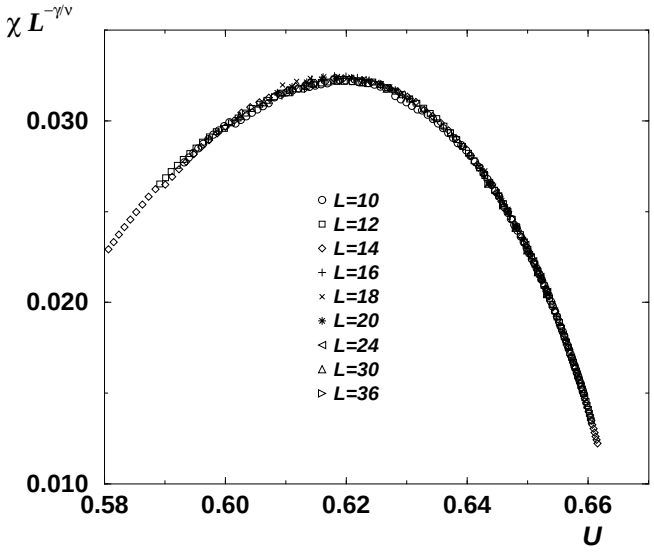
$\chi L^{-\gamma/\nu}$
0.030
0.020
0.010
0.58
0.60
0.62
0.64
0.66
U
L=10
L=12
L=14
L=16
L=18
L=20
L=24
L=30
L=36

FIG. 9.